Journal of Computational Neurocscience
in press (2003)

Spike generating dynamics and the conditions for spike-time precision in cortical neurons

Boris Gutkin[(1)], **G. Bard Ermentrout**[(2)], **Michael Rudolph**[(1)]

[(1)] Unité de Neurosciences Intégratives et Computationnelles, CNRS
UPR-2191, Bat. 33, Avenue de la Terrasse 1
91198 Gif-sur-Yvette, FRANCE

[(2)] Department of Mathematics, University of Pittsburgh,
Pittsburgh, PA, 15260, USA

February 21, 2003

Corresponding author:

Dr. M. Rudolph
Unit´e de Neuroscience Int´egratives et Computationnelles, CNRS
UPR-2191, Bat. 32-33, 1 Avenue de la Terrasse
91198 Gif-sur-Yvette
FRANCE

Tel: 33-1-69-82-34-35
Fax: 33-1-69-82-34-27
e-mail: Michael.Rudolph@iaf.cnrs-gif.fr

Abstract

Temporal precision of spiking response in cortical neurons has been a subject of intense debate. Using a canonical model of spike generation, we explore the conditions for precise and reliable spike timing in the presence of Gaussian white noise. In agreement with previous results we find that constant stimuli lead to imprecise timing, while aperiodic stimuli yield precise spike timing. Under constant stimulus the neuron is a noise perturbed oscillator, the spike times follow renewal statistics and are imprecise. Under an aperiodic stimulus sequence, the neuron acts as a threshold element; the firing times are precisely determined by the dynamics of the stimulus. We further study the dependence of spike-time precision on the input stimulus frequency and find a non-linear tuning whose width can be related to the locking modes of the neuron. We conclude that viewing the neuron as a non-linear oscillator is the key for understanding spike-time precision.

Introduction

How neurons encode sensory stimuli has been a long standing and central question of systems neuroscience. Earliest theories of neural encoding considered the mean fi ring rate as the relevant quantity (for example see Adrian and Zotterman, 1926; Barlow, 1994). However it has been long recognized that sensory information may also be encoded by the temporal pattern of the neural activity (MacKay and McCulloch, 1952). In fact, a number of recent experimental and theoretical results have suggested that coding by simple fi ring rate alone, as classically considered (e.g Barlow, 1994; see also Bugmann et al., 1997; Shadlen and Newsome, 1998; Tov´ee et al., 1993), may be at odds with observed data. Experimental studies, primarily performed in the visual system, have found a signifi cant role for precise timing of individual spikes in coding as well as precisely reproducible spike time patterns or "relational codes" (see for instance Bair and Koch, 1996; Engel et al., 1992; Krüger and Becker, 1991; McClurkin et al., 1991; Panzeri et al., 2001; Reinagel and Reid, 2000; Thorpe, 1996). This "temporal coding" hypothesis states that the precise timing of spikes, in addition to the fi ring rate, carries information (e.g. Bialek et al., 1992; Gray, 1994; Prut et al., 1998; Theunissen and Miller, 1995; for a comprehensive overview see de Charms and Zador, 2000).

A pre-requisite for the spike-time code to work is that spikes must be evoked precisely and reliably by a given stimulus. Over the past years, several converging lines of research have found that spike generation in cortical neurons can be indeed precise and reliable, depending on the nature of the inputs. In one of the fi rst experimental studies aimed at investigating mode locking and spike timing precision, Bryant and Segundo (1976) elegantly demonstrated that repeated injections of white noise in Aplysia neurons led to a remarkable invariance in the fi ring times accompanied by a high degree of reliability in the response. *In vivo* recordings have shown that the neural responses were robust and reproducible when the stimulus leads to fast fluctuations in the fi ring rates (e.g. in monkey MT: Britten, 1993; in the LGN: Reinagel and Reid, 2000) and under stimuli with statistics of natural scenes (e.g. for motion-sensitive H1 neurons in the fly's visual system: de Ruyter van Steveninck et al., 1997). *In vitro* experimental work has examined more closely the conditions for precise spike-timing (e.g Calvin and Stevens, 1968; Hunter et al., 1998; Mainen and Sejnowski, 1995; Nowak, 1997; Tang, 1997). The main fi nding of these studies is that spike-timing is rather imprecise for constant (as in Mainen and Sejnowski, 1995) and low frequency (as in Nowak et al., 1997) driving currents, but relatively precise for stimuli with pronounced temporal structure.

Precision of spike-timing has also received considerable attention in the computational literature, using a variety of modeling approaches (e.g. see Howeling et al., 2001; Needleman et al., 2001; Kretzberg et al., 2001; Van Rossum, 2001) and analytical methods (e.g. Brunel et al., 2001). In this paper we explore this issue through simulation and analysis of the stochastic θ-neuron (Gutkin and Ermentrout, 1998). While numerous models of neurons can be used for this study (e.g see Van Rossum,

2001), our choice is motivated by the fact that the θ-neuron is a reduced model of cortical neurons which captures the dynamics of neural excitability and allows for a clear distinction between the excitable and the oscillating regimes. Our main focus is to study the precision of spiking activity under noisy current inputs that reproduce in a heuristic way experimental conditions. We suggest that the experimental results (e.g Mainen and Sejnowski, 1995; Nowak et al., 1998) can be succinctly explained using the theoretical framework of non-linear oscillators, of which the θ-neuron is an example.

Methods

The Model. The model is a formal mathematical reduction from a wide class of more complicated neural models. In what follows, we briefly review its derivation. A more mathematical treatment is given in Ermentrout and Kopell (1984, 1986), Hoppensteadt and Izhikevitch (1997), Gutkin and Ermentrout (1998).

The starting point for the reduction is that the dynamical behavior of conductance based neural models is of Type I excitability (see Rinzel and Ermentrout, 1999; Hansel et al., 1995). This classification of membrane excitability was originally noted by Hodgkin in squid giant axons (Hodgkin, 1948) and is based on several characteristic properties of the neural responses to current injections. Type I neural membranes exhibit the following salient characteristics:

- All-or-none action potentials, i.e. the shape of the action potential is largely invariant with respect to the frequency of firing. In general, the amplitude and the duration of the action potential in real neurons may change slightly with the changing response frequency, but the spike remains a special and stereotyped solitary event that is well separated from the subthreshold responses. Spikes are not a continuous increase in the amplitude of subthreshold oscillations, as it would be the case for Type II membranes.
- Repetitive firing appears with arbitrarily low frequencies when the neuron is depolarized with a prolonged current step. Although this is rather difficult to observe in experiments, neural models that are parameterized to include cross-membrane conductances underlying spike generation in, for example, cortical pyramidal neurons clearly show this effect. The important notion is that the neuron is capable of responding with a wide range of firing frequencies.
- The frequency-response (f-i) curve for the Type I neuron *in vitro*, where noise levels are relatively low, can be readily fitted with a square root (for the instantaneous f-i, or the f-i for a neuron with weak spike frequency adaptation) or a linear function (the steady state f-i for a strongly adapting neuron), e.g. see Connors et al. (1990), McCormick et al. (1985), Stafstrom et al. (1984).

A majority of biophysical models for cortical neurons fall into Type I excitability. Such biophysical models have a specific underlying mathematical structure by which

the above characteristics appear, namely the saddle-node bifurcation. When analyzed in the phase space in the excitable regime (below the bifurcation) these models have at least three critical points: the attracting node that is the rest, a saddle point that is the threshold and an unstable point (repellor) that determines the shape of the action potential (see Fig.1A, left). In other words, the repellor ensures that the limit cycle traced out by the full model remains topologically invariant. The repellor persists beyond the bifurcation (see Fig.1A, right) and, thus, the action potential shape remains largely constant but the speed with which the model traverses the limit cycle changes depending on the input bias and, thus, the time between the action potentials that changes. The above characteristics of response are directly related to the structure of the bifurcation, particularly to the fact that the bifurcation occurs when the steady state (the node) comes together with the threshold (saddle point) as the injected current is increased to the critical value. As the neuron passes through the bifurcation, a single real leading eigenvalue changes its sign from negative to positive. In topological terms, right at the bifurcation there exists a single critical point and a homoclinic orbit that joins this point to itself. By definition, this orbit has infinite period (hence the arbitrarily low onset frequency) as it winds around a repellor that survives the bifurcation. Above the bifurcation the period of the oscillation is finite and the spike shape remains invariant due to the persistent repellor.

For this type of bifurcation there exists a simple canonical equation that captures the generic behavior of all models that fall within this dynamical class (see e.g. Ermentrout and Kopell, 1986 for proof):

$$\frac{d\theta}{dt} = (1-\cos\theta) + (1+\cos\theta)(\beta + I(t) + \sigma W_t), \tag{1}$$

where θ is a phase that gives the position of the neural membrane in its firing cycle. The motion of the phase is nonuniform: it is relatively slow near the rest, "speeds up" as the neural membrane traverses the spike (near $\theta = \pi$), and "slows down" during the re-polarization phase. This is the key to this model's ability to reproduce the behavior of a neural membrane, such as changes in the effective membrane time constant during spiking. The original dynamics is reduced to two phase variables due to the invariance in the shape of the limit cycle. Heuristically, since the repellor in the full model persists on both sides of the bifurcation and the limit cycle shape does not change, the firing behavior can be described by the phase around the limit cycle. Thus the repellor point is implicit in the phase description.

The input term $(\beta + I(t) + \sigma W_t)$ is multiplied by $(1+\cos\theta)$, as determined by the mathematical reduction procedure and reflecting the relative and absolute refractory periods during and after the spike. In general, the time dependent input can be of arbitrary form, with the exception of β, which is the constant bias and the major control parameter determining whether the model is below or above the bifurcation. With β below zero, the neuron is excitable and shows threshold behavior (Fig.1B, left). When the bias is positive, the neuron is in the oscillating regime producing periodic action

potentials (Fig.1B, right).

The term $I(t)$ denotes a deterministic and, in general, time varying stimulus, e.g. a constant current with amplitude α (which normally can be subsumed in the bias term), an aperiodic current or "frozen noise" (obtained from a sampled random process, or a sinusoid superimposed on a DC-offset equal to the amplitude, $I(t) = \alpha(1 + \sin(2\pi\nu_{stim}t))$. In this case, $\nu_{stim}(t)$ denotes the stimulation frequency and α the stimulation amplitude. The different stimuli used in this paper were chosen to qualitatively reflect the various current injection protocols in the *in vitro* studies: constant currents and frozen noise (Mainen and Sejnowski, 1995), or sinusoid currents (e.g. Nowak et al., 1997). The amplitudes for the DC input were set to match the experimental firing frequencies. W_t is white noise with the noise scaling factor σ. Note that the θ-neuron with noise does not have any long-lasting slow processes and is formally a Markov process with a renewal property.

The white noise injection is capable of evoking spikes in the excitable regime, or modifying the spike times for periodic firing patterns in the oscillatory regime. In the excitable regime (Fig.1B, left) the model fires due to random threshold crossings, in the oscillatory regime (Fig.1B, right) noise modulates the intrinsic rather regular spike times. Note that the noise level is the same for both panels as is the mean firing rate, yet the excitable regime gives irregular firing, while the oscillator is much more regular. The two firing regimes are readily apparent from the interspike interval coefficient of variation C_V, defined as the ratio between the standard deviation of the interspike intervals and the mean interspike interval (Fig.1C).

For further discussion of the underlying mechanisms for the interspike interval irregularity and a heuristic discussion of the stochastic θ-neuron behavior see Gutkin and Ermentrout (1998). This model can be used to explore response properties of single neurons, as well as synaptically generated behavior of small circuits (Ermentrout et al., 2001; Gutkin et al., 2001) and large synaptically coupled networks (Latham et al., 2000).

Figure 1 here

Simulation parameters. The model was run under several stimulus conditions with random initial conditions (variance of $\theta(0)$ was 10% around rest values) to model random membrane drifts seen under experimental conditions. Parameters varied during the simulations were σ, β and input stimulus characteristics as described below. The strength of the noise σ was adjusted as a free parameter. In general, the noise level fell into two qualitative classes. For "low noise", σ was chosen sufficiently small as not to affect the mean firing rate ($\sigma < 0.01$). If the cell is close to spike threshold, this situation reflects the *in vitro* constant stimulus condition in Mainen and Sejnowski (1995). For some simulations, σ was large ($\sigma > 0.01$, "strong noise"). The latter condition can be seen as one reflecting the high input levels present in *in vivo* preparations where

random synaptic inputs impinge on the neuron at a high rate (e.g. Destexhe and Par´e, 1999; Par´e et al., 1998). We note that the noise comes in our model as a current, while under *in vivo* conditions synaptic inputs are conductance fluctuations (see Discussion).

For the constant current injection, the bias β was adjusted so as to provide an average (spontaneous) firing rate consistent with previous experiments (10-40 Hz). For the time structured aperiodic stimulus we used a frozen random current. The amplitude of this stimulus was scaled as a free parameter in the simulations. For the injected sinusoid stimuli, the amplitude and frequency were changed to examine their effects on the spike-time jitter. In general, the frequency of the sinusoid was varied between 0.2 and 150 Hz, the amplitudes were set between 0 and 0.5, σ between 0 and 0.05. To ensure robust statistics, 1000 traces were simulated for each set of parameters. The model was integrated with Euler method with time step sufficiently small to ensure stability.

Data acquisition and analysis. The analysis protocol closely matches the procedure given in Mainen and Sejnowski (1995). For each parameter setup, the spiking responses for a fixed number of repetitions (in our case 1,000) of the same stimulus (constant, "frozen" random or sinusoid current) were, triggered by the stimulus onset, accumulated. The resulting rasterplots (Fig.2A) were integrated, yielding peri-stimulus time histograms (PSTHs, Fig.2B). Subtracting a threshold value (Fig.2B, threshold), which was set at the mean firing rate during the stimulus, yielded reduced PSTHs (Fig.2C). The latter can be viewed as an adequate description of the time course of the response of the cell to the applied stimulus.

Reduced PSTHs were used as input for further analysis. In most cases, the stimulation led to statistically significant peaks in the reduced PSTHs (Fig.2C), indicating the occurrence of spikes at preferred times during the course of the stimulus. In accordance with Mainen and Sejnowski (1995), these peaks in the (reduced) PSTHs are called events. A standard statistical analysis of these events was used to characterize the response with measures of reliability and precision: *Event reliability* is defined as the fraction of spikes within a single event and, thus, equals the ratio between number of spikes in a single event and the total number of spikes in the reduced PSTH (see Fig.2D). *Reliability* is the sum of the event reliability for all events occurring in the reduced PSTH, thus quantifying the fraction of total spikes specifically evoked by the stimulus. *Event jitter* is defined as the standard deviation (SD) of the spikes within a single event (Fig.2D). Finally, *precision* is defined as the average of the event precision for all events in the reduced PSTH.

Results

To determine spike time precision of the stochastic θ-neuron in the oscillatory regime, we ran a number of simulations with a constant injected current $I(t) = \alpha$. The stimulation amplitude α was set to produce repetitive firing at firing rates consistent with those previously reported in experiments (see e.g. Mainen and Sejnowski 1995). The model

was biased to oscillate in the range of 10-40 Hz frequencies ($0.1 < \alpha < 0.11$ for fixed $\sigma = 0.01$ and $\beta = -0.099$). Fig.3 shows representative results for 10 Hz and 30 Hz average firing rate. The model responds to the constant stimulus with nearly periodic spike trains. Across different trials, individual spikes are randomly shifted due to the noise. The mean firing rate, reliability and jitter can be easily matched to that observed in experiments by adjusting the noise strength σ and bias β. The PSTHs (Fig.3A) show clear peaks (events), indicating a rather regular (periodic) response. The SD of the peaks increases in the course of the stimulation (Fig.3B), leading to the "diffusion" of the events; i.e. successive events become broader and lower in amplitude, as expected for a simple renewal process. For a given noise strength, at the lower firing rates the event structure may be completely masked by the random spike-times shifts towards the end of the spike train, while for the higher firing frequencies the structure remains (results not shown). The jitter depends on the noise strength σ and decreases with increasing mean firing rate.

Figure 2 here

We then examined the response of the θ-neuron to time structured aperiodic stimuli (see Methods). Parameters, including noise, bias and initial conditions were chosen to give a mean firing rate of 10 Hz without aperiodic stimulus. Under the aperiodic stimulus the firing rate was approximately 17 Hz (Fig.3C, left). Spike times were highly correlated from trial to trial. However, in contrast to the constant stimulus, here the event jitter was not a function of the event number, but rather determined by the aperiodic input current itself (compare Fig.3C and D, right). Moreover, in the shown example, the firing rate was determined by the aperiodic stimulus and not by the bias since the background rate was 10 Hz and the "driven" rate was 17 Hz.

We can understand the above results in an intuitive way if we consider that during the constant current injection (or a slowly changing current input) the neuron is in a repetitive firing regime, i.e. the neuron produces spikes due to the intrinsic dynamics. The periodic cycling of the currents that underlies spike generation yield two distinct time scales for the evolution of the phase in the theta-neuron: the rapid all-or-none action potentials and the slow recovery (or re-polarization) of membrane excitability between the spikes. The timing of the spike depends on the duration of this slow recovery, and the membrane spends under these conditions a comparable long time in the neighborhood of the firing threshold. The presence of noise induces random changes in the recovery duration as well as random threshold crossings. Thus, in the repetitive firing regime, the noise has an expanded window of opportunity to effect individual spike times. Furthermore, previously it was shown (see Gutkin & Ermentrout, 1998) that for the Type I neurons the spike latency depends on the amplitude of input deviations above the threshold and that minute amounts of randomness in the current amplitude are amplified by the intrinsic spike generating mechanism (for ex-

perimental evidence see Azouz & Gray 1999, 2000). Thus, the repetitive fi ring regime in conjunction with noise act to induce randomness in the individual spike times.

In contrast, when the neuron is stimulated by the aperiodic stimulus (superimposed on the constant current and noise), this stimulus dominates the behavior of the membrane and the neuron fi res in response to the threshold crossings induced by the input current. Here, the neuron acts as a threshold element and the noise mechanisms discussed above are swamped by the action of the input, leading to individual spike times which are relatively robust across trials. This is in line with experimental results in Bryant and Segundo (1976), who reported reproducible and precise spike times under repeated noise injection and suggested a threshold model of the spike-triggering system.

In dynamical terms, the neuron, biased by a constant current, is a noise-perturbed nonlinear oscillator. Thus, it produces action potentials as a renewal process, meaning that the probability for the occurrence of the $(N+1)$th event depends only on two factors, namely the time of occurrence of event N and the statistics of generating an event in a given time interval.

Let us assume that the interspike interval (ISI) distribution function $P(\tau_{ISI};\mu,\sigma)$, where τ_{ISI} gives the ISI duration, is characterized by some mean μ and standard deviation σ. We can also write the moment generating function for the ISI duration $\Phi(\tau_{ISI})$, given by the Laplace transform of $P(\tau_{ISI};\mu,\sigma)$. Assuming that we have a stationary renewal process (no memory and statistical stationarity), all interspike intervals are identically distributed and independent. The time of the N-th event (spike) is the sum of the interspike intervals (τ_i) $t_N = \tau_1 + \tau_2 + \ldots + \tau_N = N\tau_{ISI}$, and the probability distribution of the N-th event time equals the N-fold convolution of the ISI distribution function:

$$P(t_N;\mu_N,\sigma_N) = P(\tau_1;\mu,\sigma) \star \ldots \star P(\tau_N;\mu,\sigma)\,. \tag{2}$$

The moment generating function for the Nth event time is:

$$\Phi(\tau_N) = \prod_{i=1}^{N} \Phi(\tau_i) = [\Phi(\tau_{ISI})]^N\,. \tag{3}$$

From this it is easy to show that the variance for the Nth event is just $N\sigma^2$. [1] Thus, standard deviation of spike times should build up as a product of the square root of the spike number and the standard deviation of the fi rst spike. Fig.3B shows plots of *event jitter* and *variance* (insets) as a function of event number. The latter follow a linear relationship, consistent with the renewal prediction. A similar relationship should hold for the experimental results (as in Mainen & Sejnowski 1995).

[1] This follows directly from the basic properties of sums of independent random variables: The distribution of the sum is characterized by the mean, which is equal to the sum of the individual means and the variance, equal to the sum of the individual variances. A simple example of this is the Poisson process where the sum of several Poisson processes is just another Poisson with the parameter (mean rate) being the sum of the individual rates (e.g. see Cox, 1979).

In contrast, for a cell driven with strong aperiodic inputs, the response appears to be evoked by the fast rising input current. The latency of the spikes is determined by the time of the current rise, and the intrinsic regenerative membrane currents are superseded. In this situation, the spike generation is not a renewal process and the precision of spike times is independent of spike number (Fig.3C).

Spike-time precision appears to be dependent on the frequency composition of the input (as found in Nowak et al. 1997). In fact, recent experiments in cortical slices suggest that certain input frequencies may be encoded preferentially, since they may be in resonance with subthreshold membrane oscillations. It was shown (Fellous et al., 2001) that *in vitro* the subthreshold dynamics of neurons may act as a band pass fi lter, allowing reliable 1 : 1 phase-locked responses to sinusoidal stimulation in a band of driving frequencies commensurate with the intrinsic oscillations.

Figure 3 here

Therefore, we next investigated the response of the θ-neuron to sinusoidal stimulation. In general, the model showed a 1 : 1 phase-locking in a broad parameter range of the driving stimulation. The occurrence of a 1 : 1 phase-locking regime was relative robust to changes in the noise strength σ and bias β, which both determine the intrinsic frequency (representative examples for low and strong noise, and driving frequencies of 10 and 30 Hz are shown in Fig.4). However, the quantitative characteristics of the locking regime depend on the model parameters. To further characterize the response, we investigated the mean output frequency ν_{out}, the jitter (precision) and reliability as a function of the driving stimulus frequency for given sets of σ and β.

Three qualitatively different regimes of phase-locking were found. First, a $1 : n$ regime, where the cell responds with several spikes during one phase of the driving stimulation ("bursts", see Fig.5A). Here, the stimulus acts as a slowly changing (or nearly constant) bias, and the output frequency during one period is mainly determined by the stimulation amplitude (Fig.6A, compare circles with triangles for $\nu_{stim} < 10$ Hz). The jitter, estimated for the whole "burst", was high (Fig.6B) and a function of the period of the stimulation. After a low reliable response for very small ν_{stim} (< 1 Hz), at higher stimulation frequencies nearly all spikes clustered into the "bursts", yielding high reliability (Fig.6C) especially in the case of low noise strength (Fig.6C, left). Interestingly, the reliability reached a plateau much earlier than the jitter, and for low noise strength the reliability value characterizing this plateau was nearly independent of the stimulation amplitude (Fig.6C, left).

An increase in the stimulation frequency leads to a rather sharp transition into the second regime, where the model 1 : 1 phase-locked to the external stimulus (see Fig.5B and the linear regime in Fig.6A). The jitter was low and nearly unaffected by the driving frequency (see plateau regions at low jitter in Fig.6B), but the value depended markedly on the intrinsic noise strength with an increasing jitter (lower precision) for

increasing noise strength (compare filled and white circles in Fig.6B). For a given noise strength, the width of the 1 : 1 regime depended mainly on the stimulation amplitude (compare white dots and triangles in Fig.6B), but was found to be rather large for a broad parameter range. For low noise amplitudes (compared to the stimulation amplitude), the behavior of the reliability as a function of the driving frequency followed that of the jitter, with a plateau region at high reliability in the 1 : 1 regime.

For strong noise strength and small stimulation amplitudes, a 1 : 1 phase-locking regime could not be observed (Fig.6A, right, filled triangles). Here, the firing rate of the model did not change with the driving frequency, and was mainly determined by the intrinsic noise amplitude and bias. The cell acted like under constant stimulation, showing events with low reliability and temporal precision (Fig.6B and C, right, filled triangles).

Figure 4 here

For increasing noise amplitudes the reliability decreased and showed a peak at stimulation frequencies comparable to the response rate with slow varying or constant stimulation of the same amplitude. Given that the average firing rate sets the threshold for estimating the reliability (see Methods), and due to the dependence of the average firing rate on the noise strength, the reliability can be viewed as a measure of the signal-to-noise ratio. For higher (but fixed) noise strength, this ratio becomes optimal (maximal) for certain stimulus characteristics, as shown here for ν_{stim}.

For further increase of the driving frequency, 1 : 1 locking is lost (stars in Fig.6B and C), as indicated by the decrease in the output rate (Fig.6A). The response of the cell in this regime was either determined by noise, or a n : 1 phase-locking was observed (Fig.5C). In the first case, no events could be seen in the PSTHs, hence no values of jitter and reliability could be deduced (filled and white triangles in Fig.6B and C). In the n : 1 phase-locking regime the model showed, for increasing stimulation frequency, a response with low jitter and decreasing reliability (for high noise, see Fig.6 filled dots), or increasing (but low) jitter and constant reliability (for low noise strength, see Fig.6 white dots). This difference between the behavior of reliability and jitter for various noise strengths can be traced back to the definitions of these two measures (see Methods). In general, as in the 1 : n regime, in the n : 1 regime the cell cannot follow the time course of the stimulation and acts like it is under constant stimulation. This is further supported by the observation that the jitter only slowly varies with increasing frequency.

Figure 5 here

In summary, our simulations of the θ-neuron show that precise and reliable spike-times in response to sinusoid stimuli are obtained in a wide range of driving frequencies. Without exhibiting strong or narrow resonances for a particular intrinsic frequency range, the cell acts like a band pass filter, in agreement with previous studies (Fellous et al., 2001). The intrinsic parameters, like the noise strength or constant bias, act as a modulating factor on the shape and width of the $1:1$ locking regime.

Discussion

In this report we have considered the reproducibility of spike timing in Type I neurons by studying the responses of the canonical model for this excitability class, the θ-neuron. First, we showed that spike timing precision and reliability results reported previously from *in vitro* experiments can be reproduced by the stochastic θ-neuron. In spike trains evoked by constant current injections (oscillating regime, Fig.3A and B), the overall spike-time jitter is high and increases with successive spikes. Here the response is caused by regenerative activity of the intrinsic currents and the jitter in each spike depends on the jitter in the preceding spikes. On the other hand, under aperiodic stimulus (Fig.3C), the response is caused by the rapid fluctuations in the stimulus itself, and the cell acts as an excitable threshold element. In this case, a given spike is largely statistically independent from the previous spike and its jitter is stationary and relatively low compared to the constant case with constant stimulation.

We tested the hypothesis that spike timing precision is strongly affected by the temporal structure of the stimulus. The simulations with sinusoid input showed that slow rising stimuli act almost like an additional bias and result in imprecise spike times. Rapid stimuli (frequencies above 100 Hz) are filtered by the membrane and once again lead to low precision (Fig.5C). In between both regimes, there was a wide optimal range of input frequencies that evoke precisely timed spikes (Fig.5B and 5). No sharp resonances with respect to intrinsic frequencies were found, but a rather broad band pass filter behavior. This is predicted from the dynamics of Type I membrane excitability and is quite different from the situation described in studies of noise driven Type II oscillators (e.g. Jensen, 1998). In the latter case, each oscillator exhibits subthreshold oscillations in a limited frequency band, leading to a narrow range of periodic inputs that evoke precisely timed responses.

Fellous et al. (2001) showed *in vitro* that the precision tuning in prefrontal cortical neurons can be correlated with subthreshold oscillations of the membrane potential. A broad tuning curve for the reliability of the response to sinusoid current stimuli at a frequency corresponding to the average subthreshold oscillation frequency was found. Although there are no subthreshold oscillations in the theta-neuron model, we obtain results that qualitatively match these experimental findings. In addition, no sharp differences in the precision and reliability tuning could be deduced between the cases where the constant stimulus amplitude was below the oscillatory regime (thus, the cell operated in the excitable regime) and those in the oscillatory regime (see Methods).

This suggests that the stated link between subthreshold oscillations and reliability of the cellular response might be weaker. Also, the broad reliability tuning found experimentally appears to be in contrast with a sharp tuning one expects for a resonance coupling between subthreshold oscillations and response, indicating that the subthreshold neuronal dynamics is not the only determinant of a reliable response under the investigated current stimuli.

The loss of precise spike-timing in the model for higher input frequencies can be explained by the structure of the stable locking regimes of non-linear oscillators (e.g see Coombes and Bresloff, 1999). That is, the precision and reliability tuning curves have their inflection points at the frequency where 1:1 locking mode is lost. For Type I oscillators this upper bound is dependent on the input amplitude (as it would be for any non-linear oscillator), and also on the amplitude of the back-ground DC component of the input. Thus, we predict that it is the upper edge of the tuning that would be modified by the input amplitude or the DC off-set.

The response rate of the model as a function of the stimulus frequency shows that, in the $1:1$ phase-locking regime, the cell phase-locked to the external stimulus by modulating its firing rate. The firing rate sharply decreased at a critical frequency, indicating the loss of a reliable and precise response to the external stimulus. This behavior is typical for current driven (noise or stimulus) models. Simulations performed using simplified models of cortical neurons with voltage-dependent membrane conductances and synaptic background activity modeled either by current or conductance noise (Destexhe et al., 2001) revealed two different modes of $1:1$ phase-locking. Whereas under current noise the neuron encoded different stimuli by modulating its firing frequency, under conductance noise the relative timing of spikes was changed with only minimal impact on the mean output rate (Rudolph and Destexhe, unpublished observation). High-frequency stimuli (up to 200 Hz) could be resolved for a broad parameter range with high precision and reliability with conductance noise (Rudolph and Destexhe, 2002), but not with current noise. The latter is in agreement with the breakdown of a precise response for higher driving frequencies ($\nu_{stim} > 70$ Hz) reported here. The difference between both locking modes can be traced back to the high conductance component imposed by synaptic background activity, and the resulting decrease of the effective membrane time constant. To which extent the noisy component σ in the stochastic θ-neuron model used in the present study describes synaptic background activity remains to be investigated.

We have shown that the θ neuron model reproduces experimental results which suggest that the precisely timed spiking is primarily a result of rapidly changing inputs driving the cell to spike threshold. This particular fact has already been recognized by Bryant and Segundo (1976) in an experimental study of Aplysia neurons *in vitro*. The authors found that in response to repeated injection of Gaussian white noise the neuron responded with highly reproducible spike trains. After estimating the first order Wiener kernel for the neuron (or the average current input leading to spike production), Bryant and Segundo were able to heuristically account for this effect of noise injection by a simple current threshold device coupled with this kernel. In our study

we looked into this issue by quantifying the precision of spike timing for individual spikes. We also found that, in this mode, the neuron's response can be described best in terms of a thresholding effect, provided that spike-generating dynamics are taken into account. Interestingly, Bryant and Segundo found that the average input leading to a spike depended on the DC input bias, with more depolarized bias yielding input waveforms that included an early hyperpolarizing component, followed by a rapid depolarizing component. This is compatible with our conjecture (see Results) that a neuron that is sitting near its firing threshold would need to be transiently re-polarized in order to remove any partial inactivation of the sodium channels and, thus, augment the membrane excitability. Such re-polarization would break any remaining effects of the previous spike or, in other words, transiently move the cell out of the oscillating regime and, hence, result in a reliable spike timing. At more hyperpolarizing bias the cell is away from the threshold and, thus, already in the excitable (threshold) regime, with no requirement of an additional hyperpolarization.

A crucial difference between the elegant early study by Bryant and Segundo (1976) and the work presented here is that Bryant and Segundo essentially approached spike generation as a thresholding process. In this study we suggest a specific dynamical structure for spike generation (Type I dynamics). We show that it is able to account for responses of neurons to a variety of noisy stimuli (DC and noise, repeated noise, sinusoid current and noise) quantitatively and also provide a unifying explanation for such responses. Furthermore, the focus of the study by Bryant and Segundo (1976) was different by asking what input patterns lead to spikes and how such pattern can be characterized by estimating first and second order Wiener kernels. We drew attention more on the question wether a canonical model of spike generation can account for spike time precision and reliability and how these can be explained in the context of non-linear oscillators.

In fact we propose that spike timing is a microscopic quantity that reflects strongly the fine temporal structure of the input current (i.e. high frequency fluctuations, possibly due to correlation structure in the synaptic inputs as discussed in Salinas and Sejnowski, 2000). On the other hand bias induced firing preserves the over-all firing rate, a macroscopic quantity that depends on the mean level of the input current. In this way we may imagine that the firing rate and the spike timing can be multiplexed to carry two related but different kinds of information about a sensory stimulus. It is interesting to note that when the spike-times are precise across trials, the ISIs within an individual spike train are highly variable (C_V near 1, results not shown). In fact, there is a reciprocal relationship between the ISI coefficient of variation and the spike time jitter (see Gutkin & Ermentrout 1998 for further discussion). Thus, we suggest that the high C_V observed *in vivo* is a signature of precise spike-timing, whereas a more regular discharge activity indicates that the neuron acts as an oscillator.

In this report we have not considered the effect of slower intrinsic currents, such as currents causing spike-frequency adaptation. The latter would increase variability as a consequence of the "forward excitability break" proposed by Wang (1998), and change the renewal explanation given here for the constant current case (see Results). The

simple picture we presented is a minimal case. Our modeling conditions correspond roughly to the experiments of Tang (1997) where the slow potassium channels were blocked by acetylcholine. This manipulation appeared not to affect the overall precision of a given spike-train. The slow currents may induce subthreshold resonances on the membrane potential by converting Type I behavior into Type II (as shown in Ermentrout et al., 2001). Signatures of resonances have been shown experimentally in Aplysia neurons (see Hunter et al., 1998). In that study, the resonance in spike-time jitter was shown to be directly related to the resonant frequency of the stimulated neuron. The relationship between the input frequency tuning and the effects of spike frequency adaptation on the membrane resonances remains to be investigated.

Another issue that remains to be investigated is how the synaptic identity of the inputs affects the spike time precision (in this report we only considered current stimuli). Our results imply that rapid fluctuations in the inputs are crucial for spike-time precision. Such rapid input fluctuations could be a result of correlated bursts of rapid excitatory synapses, e.g. AMPA receptors, while the lower frequencies could be either due to asynchronous synaptic activity or slower NMDA receptors. Recently, Harsch & Robinson (2000) have shown that spike-time precision is lower for NMDA-like inputs than for AMPA postsynaptic potentials. Furthermore, it was shown that for each NMDA evoked burst of action potentials the initial spikes are precise, while the trailing spikes are imprecise. This is in agreement with the behavior obtained in simulations with the θ-neuron for low frequency sinusoids, where the cell fires many spikes per stimulus cycle. Thus, the theoretical model presented here is sufficient to give a simple explanation of the experimental results: The initial spike in each burst is caused by the stimulus crossing the threshold, whereas the subsequent spikes are evoked by the intrinsic spiking mechanism. The resulting average precision should then be lower for NMDA stimuli.

Another way to obtain rapid fluctuations in the input current is through random activation of inhibitory synapses. In fact, Harsch & Robinson (2000) reported that the presence of inhibitory inputs significantly improved spike-time precision. Interpreted in our framework this means that the inhibitory inputs provide rapid hyperpolarizing transients and "reset" the neuron (for example by removing inactivation of the sodium channels and/or activation of slow potassium channels), thus breaking the oscillatory serial dependence between successive spikes.

In conclusion, by using the θ-neuron, we have tied specific experimental results to a structural mathematical theory of the nonlinear dynamics of spike generation. Since the θ-neuron is the canonical model for Type I membrane excitability, the results presented here should apply to neural models as long as they exhibit Type I dynamics. To which extend our results apply to more complex neural models, e.g. those with extended dendritic structures, voltage dependent conductances that modulate the dynamics of spike generation and conductance inputs, remains an interesting subject for future investigations.

Acknowledgments

This work was supported by the NSF Biological Informatics Fellowship (BSG) and CNRS (MR). We thank Yves Fr´egnac and Alain Destexhe for valuable discussions and support of this work.

References

1. Adrian E D, Zotterman Y (1926) The impulses produced by sensory nerve endings. Part.2. The response of a single end organ. *J Physiol* 61: 151-171.

2. Azouz R, Gray C M (1999) Cellular mechanisms contributing to response variability of cortical neurons in vivo. *J. Neuroscience* 19: 2209-2223.

3. Azouz R, Gray C M (2000) Dynamic spike threshold reveals a mechanism for synaptic coincidence detection in cortical neurons in vivo. *Proc. Natl. Acad. Sci. USA* 97: 8110-8115.

4. Bair W, Koch C (1996) Temporal precision of spike trains in extrastriate cortex of the behaving macaque monkey. *Neural Comp.* 8: 1185-1202.

5. Barlow H (1994) The neuron doctrine in perception. In: The Cognitive Neuroscience (ed. M. Gazzaniga). MIT Press, Boston: 415-435.

6. Bialek W, Rieke F (1992) Reliability and information transmission in spiking neurons. *Trends. Neurosci* 15: 428-434.

7. Bishop P O, Levick W R, Williams W O (1964) Statistical analysis of the dark discharge of lateral geniculate neurones. *J. Physiol.* 170: 598-612.

8. Britten K H, Shadlen M N, Newsome W T, Movshon J A (1993) Response of neurons in macaque MT to stochastic motion signals. *Visual Neurosci.* 10: 1157-1169.

9. Brunel N, Chance F S, Fourcard N, Abbott L F (2001) Effects of Synaptic Noise and Filtering on the Frequency Response of Spiking Neurons. *Phys. Rev. Lett.* 86: 2186-2189.

10. Bryant H L, Segundo J P (1976) Spike initiation by transmembrane current: A white-noise analysis. *J. Physiol.* 260: 279-314.

11. Bugmann G, Christodoulou C, Taylor J G (1997) Role of temporal integration and fluctuation detection in the highly irregular fi ring of a leaky integrator neuron model with partial reset. *Neural Comp.* 9: 985-1000.

12. Calvin W H, Stevens C F (1968) Synaptic noise and other sources of randomness in motoneuron interspike intervals. *J. Neurophysiol.* 31: 574-587.

13. Connors B W, Gutnick M J (1990) Intrinsic fi ring patterns of diverse neocortical neurons. *Trends Neurosci.* 13: 99-104.

14. Coombes S, Bressloff P (1999) Mode locking and Arnold tongues in integrate-and-fi re neural oscillators. *Phys. Rev. E* 60: 2086-2096.

15. Cox D R (1970) Analysis of Binary Data. London: Chapman and Hall.

16. de Charms R C, Zador A (2000) Neural representation and the cortical code. *Annu. Rev. Neurosci.* 23: 613-647.

17. de Ruyter van Steveninck R R, Strong S P, Koberle R, Bialek W (1997) Reproducibility and variability in neural spike trains. *Science* 275: 1805-1808.

18. Destexhe A, Par´e D (1999) Impact of network activity on the integrative properties of neocortical pyramidal neurons in vivo. *J. Neurophysiol.* 81: 1531-1547.

19. Destexhe A, Rudolph M, Fellous J-M, Sejnowski T J (2001) Fluctuating synaptic conductances recreate in vivo-like activity in neocortical neurons. *Neurosci.* 107: 13-24.

20. Engel A K, König P, Kreiter A K, Schillen T B, Singer W (1992) Temporal coding in the visual cortex: new vistas on integration in the nervous system. *Trends Neurosci.* 15: 218-26.

21. Ermentrout G B, Kopell N K (1984) Frequency plateaus in a chain of weakly coupled oscillators I. *SIAM J. Math. Analysis* 15: 215-237.

22. Ermentrout G B, Kopell N K (1986) Parabolic bursting in an excitable system coupled with a slow oscillation. *SIAM J. Appl. Math.* 46: 233-253.

23. Ermentrout G B, Pascal M, Gutkin B (2001) The effects of spike frequency adaptation and negative feedback on the synchronization of neural oscillators. *Neural Comp.* 13: 1285-1310.

24. Fellous J-M, Howeling A R, Modi R H, Rao R P N, Tiesinga P H E, Sejnowski T J (2000) Frequency dependence of spike timing reliability in cortical pyramidal cells and interneurons. *J. Neurophys.* 85: 1782-1787.

25. Gutkin B S, Ermentrout G B (1998) Dynamics of membrane excitability determine interspike interval variability: a link between spike generation mechanisms and cortical spike train statistics. *Neural Comp.* 10: 1047-1065.

26. Gutkin B S, Laing C, Colby C, Chow C C, Ermentrout G B (2001) Turning on and off with excitation: the role of spike-timing synchrony and asynchrony in sustained neural activity. *J. Comp. Neurosci.* 11: 121-134.

27. Gray C M (2000) Synchronous oscillations in neuronal systems: mechanisms and functions. *J. Comp. Neurosci.* 1: 11-38.

28. Hansel D, Mato G, Meunier C (1995) Synchrony in excitatory neural networks. *Neural Comp.* 7: 307-337.

29. Harsch A, Robinson H P C (2000) Postsynaptic variability of fi ring in rat cortical neurons: the role of input synchronization and synaptic NMDA receptor conductance. *J. Neurosci.* 20: 6181-6192.

30. Hodgkin A L (1948) The local changes associated with repetitive action in nonmedulated axon. *J. Physiol.* 107: 165-181.

31. Hoppensteadt F, Izhikevich E (1997) Weakly Connected Neural Nets. Springer-Verlag, Berlin.

32. Howeling A R, Modi R H, Granter P, Fellous J-M, Sejnowski T J (2001) Models of frequency preferences of prefrontal cortical neurons. *Neurocomputing* 38: 231-238.

33. Hunter J D, Milton J G, Thomas P J, Cowan J D (1998) Resonance effect for neural spike time reliability. *J. Neurophysiol.* 80: 1427-1438.

34. Jensen R, Jones L, Gartner D H (1998) Synchronization of randomly driven nonlinear oscillators and the reliable fi ring of cortical neurons. In: Computational Neuroscience: Trends in Research 1998 (ed. J.M.Bower). New York: Plenum.

35. Kretzberg J, Egelhaaf M, Warzecha A K (2001) Membrane potential fluctuations determine the precision of spike timing and asynchronous activity: A model study. *J. Comp. Neurosci.* 10: 79-97.

36. Krüger J, Becker J D (1991) Recognizing the visual stimulus from neuronal discharges. *Trends Neurosci.* 14: 282-286.

37. Latham P E, Richmond B J, Nelson P G, Nirenberg S (2000) Intrinsic dynamics in neuronal networks. I. Theory. *J. Neurophysiol.* 83: 808-827.

38. MacKay D, McCulloch W (1952) The limiting information capacity of a neuronal link. *Bull. Math. Biophys.* 14: 127-135.

39. Mainen Z F, Sejnowski T J (1995) Reliability of spike timing in neocortical neurons. *Science* 268: 1503-1506.

40. McClurkin J W, Optican L M, Richmond B J, Gawne T J (1991) Concurrent processing and complexity of temporally encoded neuronal messages in visual perception. *Science.* 253: 675-677.

41. McCormick D A, Connors B W, Lighthall J W, Prince D A (1985) Comparative electrophysiology of pyramidal and sparsely spiny stellate neurons of the neocortex. *J. Neurophysiol.* 54: 782-806.

42. Nowak L G, Sanchaez-Vives M V, McCormick D A (1997) Influence of low and high frequency inputs on spike timing in visual cortical neurons. *Cerebral Cortex* 7: 487-501.

43. Needleman D J, Tisienga P H E, Sejnowski T J (2001) Collective enhancement of precision in networks of coupled oscillators. *Physica D* 155: 324-336.

44. Panzeri S, Petersen R S, Schultz S R, Lebedev M, Diamond M E (2001) The role of spike timing in the coding of stimulus location in rat somatosensory cortex. *Neuron* 29: 769-777.

45. Par´e D, Shrink E, Gaudreau H, Destexhe A, Lang E J (1998) Impact of spontaneous synaptic activity on the resting properties of cat neocortical pyramidal neurons in vivo. *J. Neurophysiol.* 79: 1450-1460.

46. Prut Y, Vaadia E, Bergman H, Haalman I, Slovin H, Abeles M (1998) Spatiotemporal structure of cortical activity: properties and behavioral relevance. *J. Neurophysiol.* 79: 2857-2874.

47. Reinagel P, Reid R C (2000) Temporal coding of visual information in the thalamus. *J Neurosci.* 20: 5392-5400.

48. Rinzel J M, Ermentrout G B (1998) Analysis of Neuronal Excitability, in Methods in Neuronal Modeling, 2nd edition C. Koch and I. Segev, eds, MIT Press Cambridge, MA.

49. Rudolph M, Destexhe A (2002) Gain modulation and frequency locking under conductance noise. CNS 2002 Abstract.

50. Salinas E, Sejnowski T J (2000) Impact of correlated synaptic input on output fi ring rate and variability in simple neuronal models. *J. Neurosci.* 20: 6193-6209.

51. Shadlen M, Newsome W T (1998) The variable discharge of cortical neurons: implications for connectivity, computation, and information coding. *J. Neurosci* 18: 3870-3896.

52. Stafstrom C E, Schwindt P C, Crill W E (1984) Repetitive fring in layer V neurons from cat neocortex in vitro. *J. Neurophysiol.* 52: 264-277.

53. Tang A (1997) Effects of cholinergic modulation on responses of neocortical neurons to fluctuating input. *Cereb. Cortex* 7: 502-509.

54. Teich M C, Henegan C, Lowen S B, Ozaki T, Kaplan E (1997) Fractal character of the neural spike train in the visual system of the cat. *J. Opt. Soc. Am.* 14: 529-546.

55. Theunissen F, Miller J P (1995) Temporal encoding in nervous systems: a rigorous defi nition. *J. Comp. Neurosci.* 2: 149-162.

56. Thorpe S, Fize D, Marlot C (1996) Speed of processing in the human visual system. *Nature* 381: 520-522.

57. Tovee M J, Rolls E T, Treves A, Bellis R P (1993) Information encoding and the responses of single neurons in the primate temporal visual cortex. *J. Neurophysiol.* 70: 640-654.

58. Van Rossum M C W (2001) The transient precision of integrate and fi re neurons: effects of background activity and noise. *J. Comp. Neurosci.* 10: 303-311.

59. Wang X-J (1998) Calcium coding and adaptive temporal computation in cortical pyramidal neurons. *J. Neurophysiol.* 79: 1549-1566.

Figure Captions

Figure 1 The θ-neuron model. **A**: Representative Type I membrane dynamics (Morris-Lecar model). $V - w$ phase plots, where V denotes the membrane potential and w the recovery variable (see Rinzel and Ermentrout, 1998), are shown for the excitable (left panel) and oscillatory (right panel) regime. In the excitable regime, w-nullclines (grey solid) and V-nullclines (grey dashed) intersect at three points: a stable resting state (R), a saddle point threshold (T) and an unstable node (U). Unstable and stable manifolds for the saddle node are indicated by black solid and dashed lines, respectively. Lifting the V-nullcline by a constant bias current, one observes a bifurcation of the critical points in the course of which the resting state and saddle node disappear, leaving only the unstable node. The topology of the transient orbits due to suprathreshold excitation in the excitable regime and the stable limit cycle in the oscillatory regime remains invariant. This invariance allows for a reduction to the phase description. **B**: Scheme of the dynamical structure of the θ-neuron, shown in the excitable regime ($\beta < 0$, left) and the oscillatory regime ($\beta > 0$, right). The relative positions of the rest and the threshold are determined by β; the spike occurs near $\theta = \pi$, where the rate of change of the phase is the fastest and the inputs are "shunted". If β is adjusted above zero, the model passes into an oscillatory regime, where the spikes are produced due to intrinsic oscillations. The unstable node is implicit in the formulation of the θ-neuron. The insets show representative (spontaneous) activity of the θ-neuron in the excitable regime due to random noise inputs, and oscillatory regime due to intrinsic mechanisms. Here, β is adjusted so as to produce mean firing at 10 Hz in both cases, $\sigma = 0.01$. Note that here we plot an auxiliary quantity $\nu = 1 - \cos\theta$ in order to visualize spikes. **C**: Coefficient of variation (C_V) as a function of model parameters β and σ. The C_V quantifies the regularity of the train of individual events, and shows the two regimes characterizing the θ-neuron: Whereas regular spiking activity (oscillatory regime) yields low C_V values, for irregular activity the C_V is around 1.

Figure 2 Simulation and data analysis protocol. The responses of the θ-neuron to repeated stimulation with fixed stimuli (see Methods) were recorded. The resulting rasterplots (**A**) were integrated, yielding peri-stimulus time histograms (PSTHs) with spike times clustering into contiguous groups of bins (**B**). After a further reduction of the PSTHs by cutting above a threshold which corresponds to the mean firing rate during the stimulus (yielding reduced PSTHs, see **C**), these groups define events of enhanced occurrence of spikes in the course of the stimulus (see peaks in **C**). The number of spikes falling into a single event as well as the standard deviation (SD) of the spike times belonging to a single event yield event reliability and event jitter, respectively (**D**). The average of the event jitter and the sum of the event reliability for all events observed during the stimulation finally define jitter and reliability used in the analysis.

Figure 3 Spike timing jitter under constant current injection is compatible with a renewal process. The jitter grows as a square root of the event number (variance is proportional to event number), and is reduced for higher fi ring rates. **A**: Typical rasterplots (upper panels) and PSTHs (lower panels) for constant stimuli. The bias was adjusted to give 10 Hz (left) and 30 Hz (right) average fi ring rate. The noise strength was fi xed to $\sigma = 0.001$. **B**: Spike-time jitter and spike-time variance (insets) as a function of the event number. Left: Result for mean fi ring rate of 10 Hz and noise amplitude of $\sigma = 0.001$ (stars) and $\sigma = 0.003$ (dots). Right: Results for $\sigma = 0.001$ (stars) and $\sigma = 0.003$ but higher bias (average fi ring rate 30 Hz). **C**: Example of spike-time jitter in the θ-neuron under an aperiodic stimulus. Left: rasterplots (upper panel) and PSTH (middle) for repeated injection of aperiodic current (lower panel; mean fi ring rate 17 Hz, amplitude of aperiodic stimulus 0.05, noise strength $\sigma = 0.003$). Right: jitter as function of even number. Note that under such strong aperiodic signal the event jitter does not depend on event number.

Figure 4 Representative responses of the θ-neuron to sinusoidal stimuli. Rasterplots (top panels) and PSTHs (bottom panels) for sinusoid injections of a fi xed amplitude $\alpha = 0.045$ and frequency of 10 Hz (**A, C**) and 30 Hz (**B, D**) for two different noise strength (**A, B**: $\sigma = 0.003$ low noise, **C, D**: $\sigma = 0.05$ strong noise) are shown ($\beta = -0.099$). The mean frequency in the presence of stimulation is marked on the graphs, and was different from the intrinsic frequency without stimulation (10 Hz). In all cases, the cell phase-locked to the driving stimulus.

Figure 5 Rasterplots and the PSTHs for three different stimulation frequencies (parameters: $\alpha = 0.09$, $\beta = -0.099$, $\sigma = 0.003$ weak noise, see also Fig.6), indicating three locking regimes: Low and high driving frequencies (upper and lower panel, respectively) act like a constant bias, whereas for intermediate driving frequencies (middle panel) the model phase-locked with a high temporal resolution to the driving stimulus.

Figure 6 Mean output rate ν_{out} (**A**), jitter (**B**) and reliability (**C**) as a function of the frequency ν_{stim} of the sinusoidal stimulation for weak (left) and strong (right) noise strength. Representative results for two stimulation amplitudes (dots: $\alpha = 0.09$, triangles: $\alpha = 0.01$) and two different noise strength (white symbols: $\sigma = 0.003$ low noise; fi lled symbols: $\sigma = 0.5$ strong noise) are shown ($\beta = -0.099$). The arrows in the upper right panel mark stimulation frequencies for which rasterplots and PSTHs are shown in Fig.5. Stars in the precision and the reliability plots mark the frequency at which $1:1$ phase-locking is lost, or at which the model can no longer resolve the stimulus. Note that for the weak stimulus the tuning in both precision and reliability is rather narrow, while for the strong stimulus the tuning is wide. The upper limit of the tuning in both cases is related to the critical input frequency at which 1:1 locking begins to deteriorate.

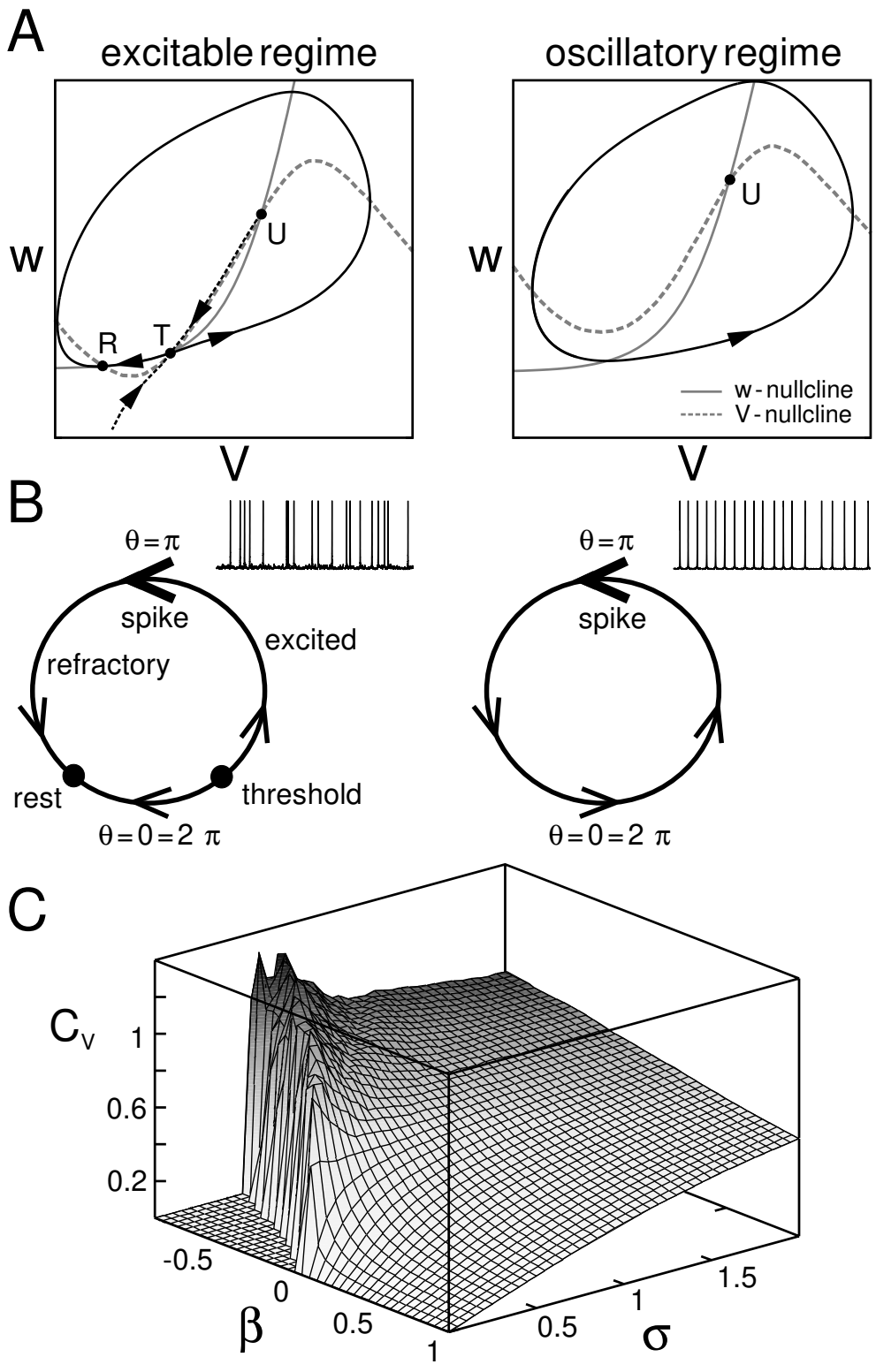
A
excitable regime
oscillatory regime
w
U
R
T
V
w - nullcline
V - nullcline
B
θ = π
spike
excited
refractory
rest
threshold
θ = 0 = 2 π
C
C_V
1
0.6
0.2
-0.5
0
0.5
1
β
0.5
1
1.5
σ

Figure 1

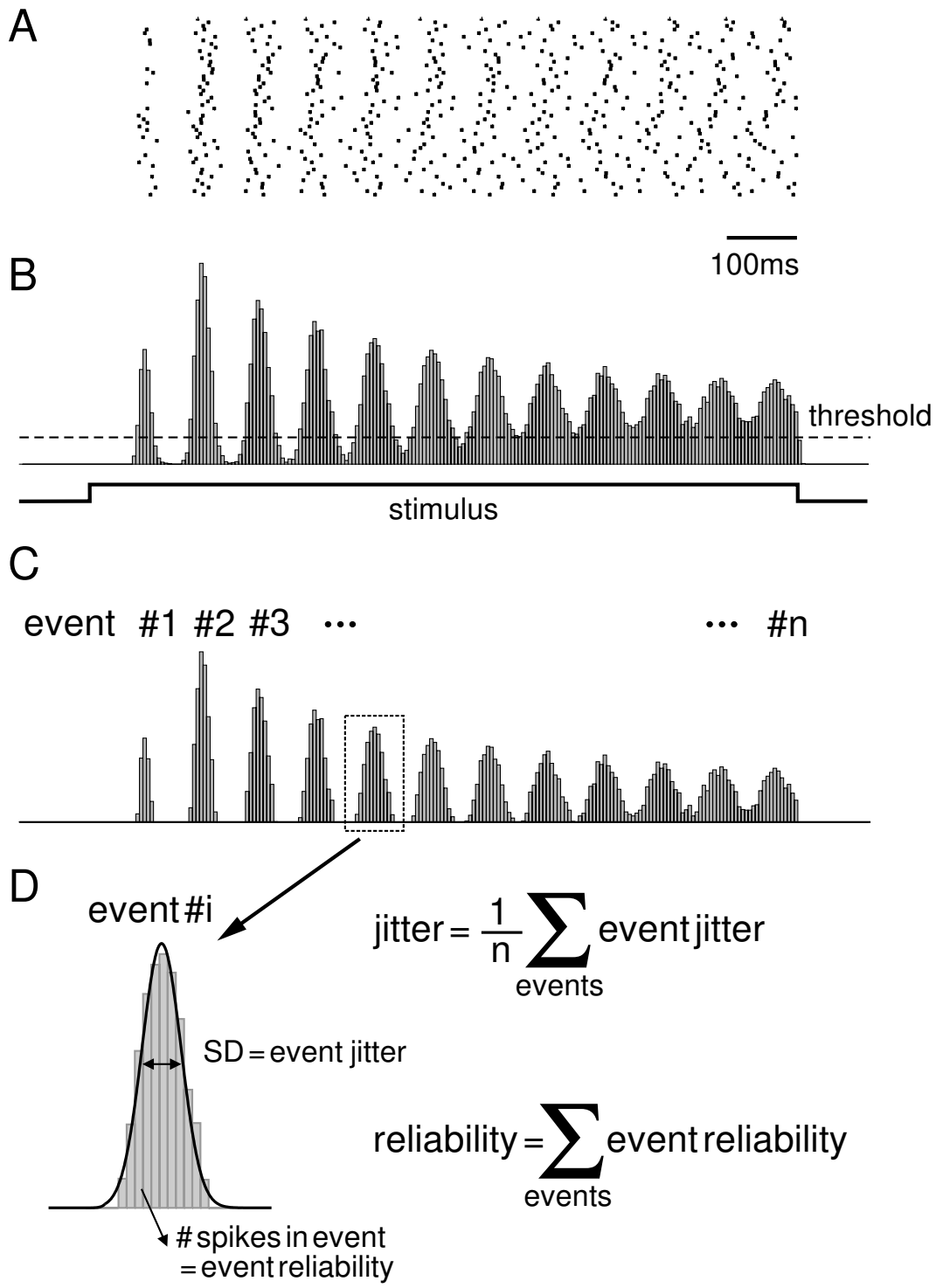
A
100ms
B
threshold
stimulus
C
event #1 #2 #3 ••• ••• #n
D
event #i
jitter = 1/n ∑ events event jitter
SD = event jitter
reliability = ∑ events event reliability
# spikes in event
= event reliability

Figure 2

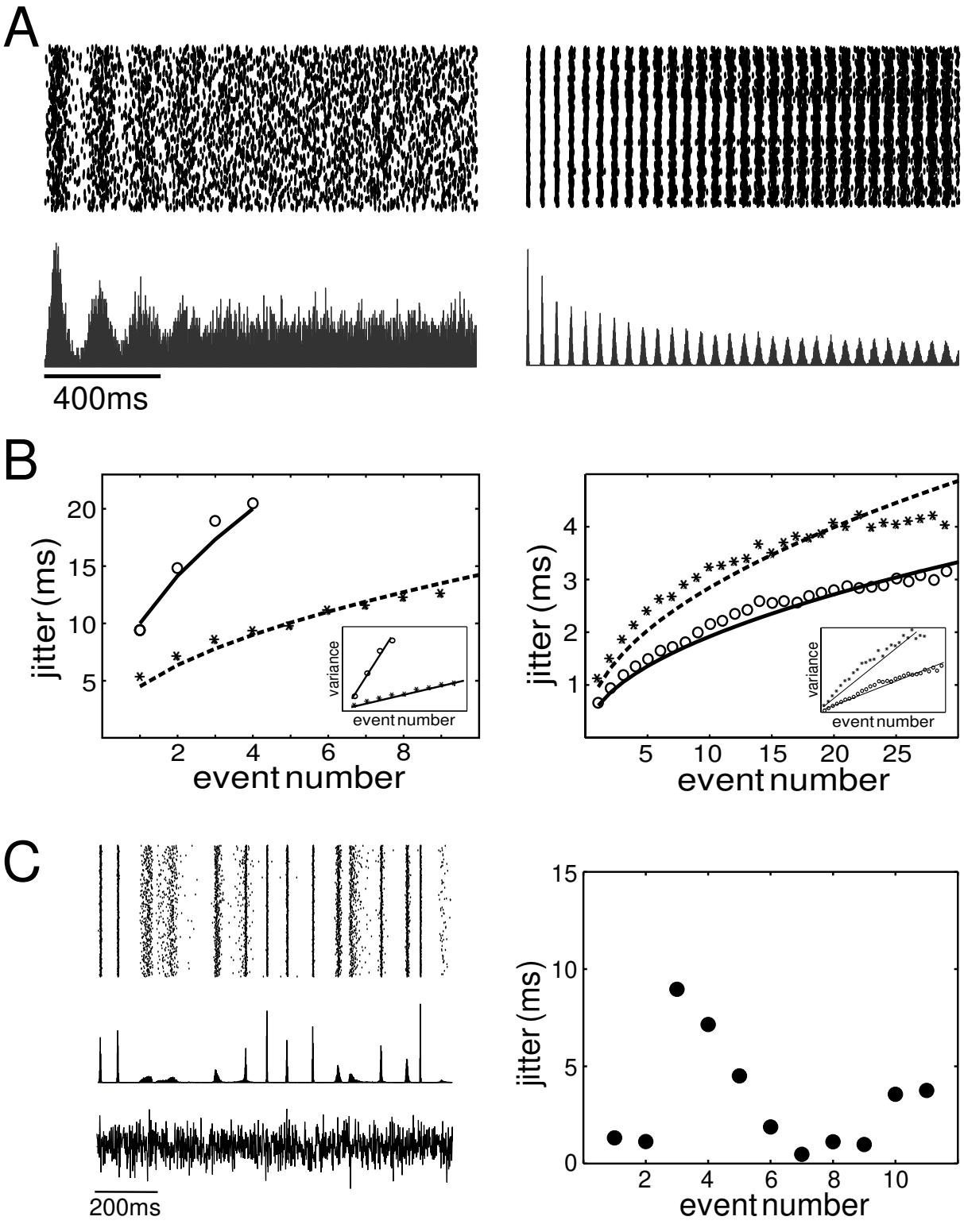
A
400ms
B
jitter (ms)
event number
variance
event number
C
200ms
jitter (ms)
event number

Figure 3

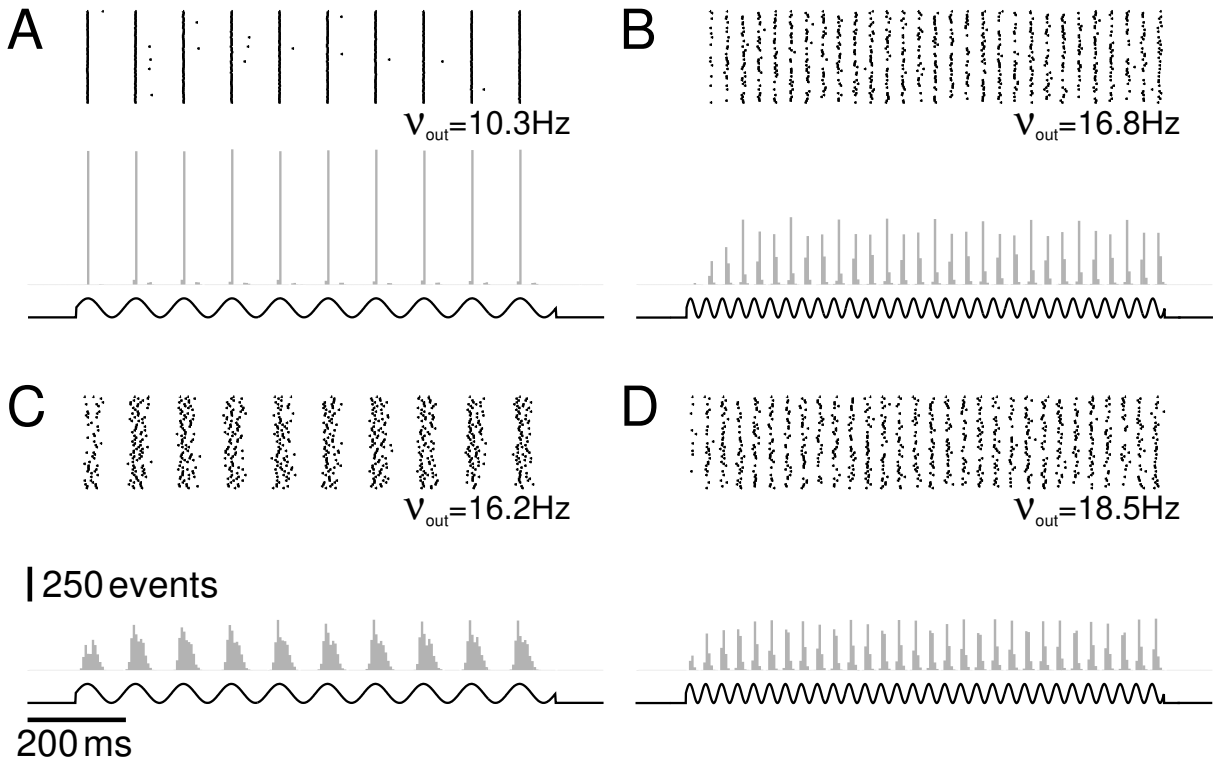
A
ν_{out}=10.3Hz
B
ν_{out}=16.8Hz
C
ν_{out}=16.2Hz
D
ν_{out}=18.5Hz
250 events
200 ms

Figure 4

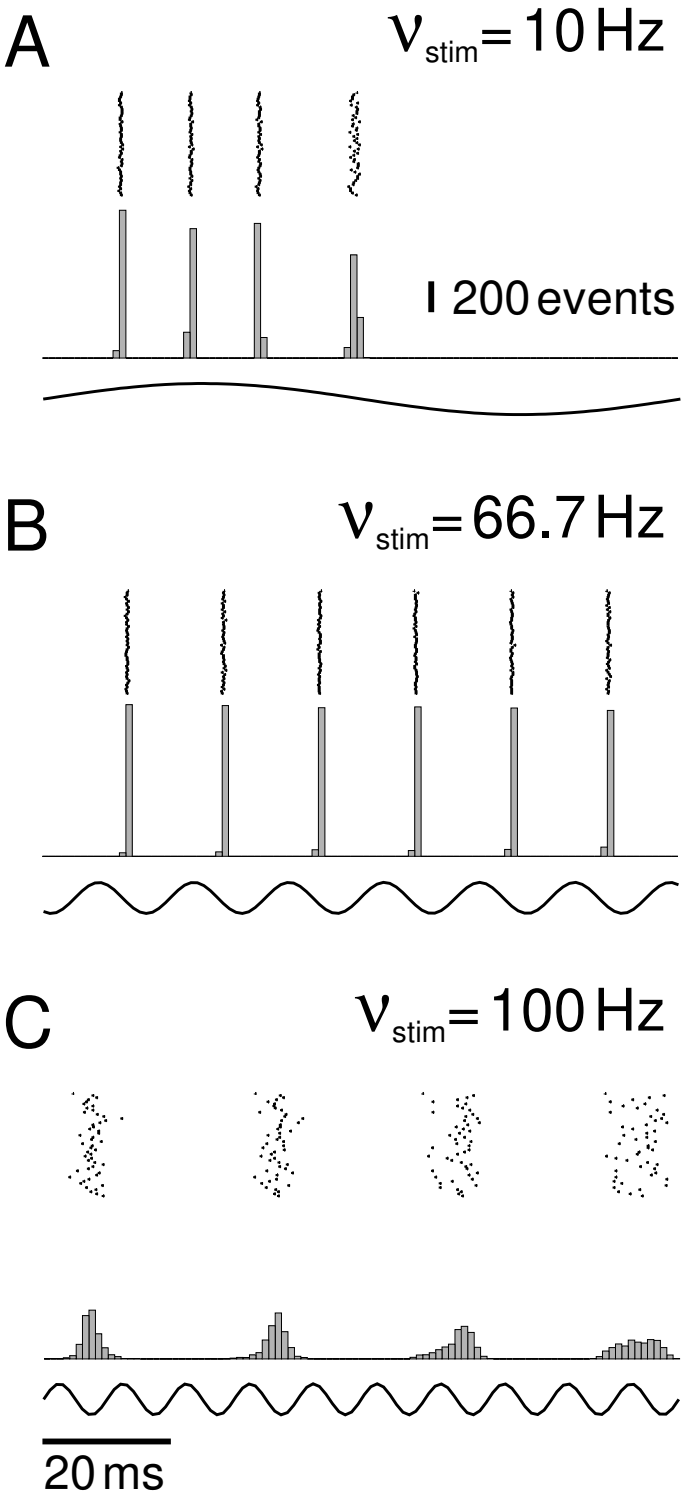

Figure 5

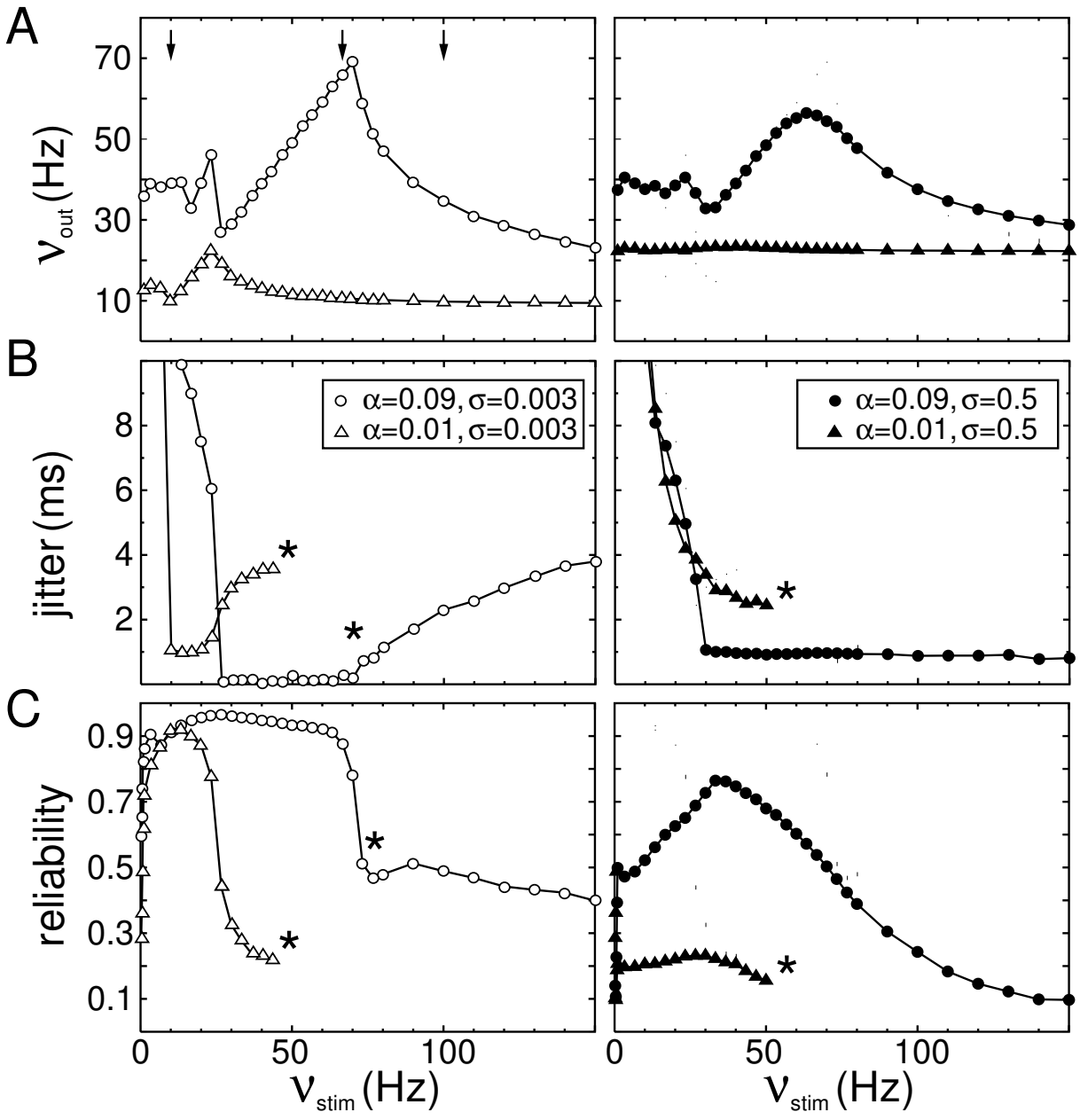
A
B
C
70
50
30
10
ν_{out} (Hz)
8
6
4
2
jitter (ms)
α=0.09, σ=0.003
α=0.01, σ=0.003
α=0.09, σ=0.5
α=0.01, σ=0.5
0.9
0.7
0.5
0.3
0.1
reliability
0
50
100
ν_{stim} (Hz)

Figure 6